Stromal Fibroblast–Specific Expression of ADAM-9 Modulates Proliferation and Apoptosis in Melanoma Cells *In Vitro* and *In Vivo*

Anna N. Abety[1], Jay W. Fox[2], Alexander Schönefuß[1], Jan Zamek[1], Jenny Landsberg[3], Thomas Krieg[1], Carl Blobel[4], Cornelia Mauch[1] and Paola Zigrino[1]

ADAMs are members of the zinc metalloproteinase superfamily characterized by the presence of disintegrin and metalloprotease domains. In human melanoma, ADAM-9 is expressed in focalized areas of the tumor–stroma border in both melanoma and stromal cells. However, the role of ADAM-9 in melanoma progression remains elusive. To analyze the role of stromal-derived ADAM-9 for the growth and survival of melanoma cells, we have used *in vitro* coculture systems of melanoma cells and ADAM-9$^{-/-}$ fibroblasts. Coculture of melanoma cells in the presence of ADAM-9$^{-/-}$ fibroblasts led to increased melanoma cell proliferation and reduced apoptosis as compared with control cocultures. We identified TIMP-1 and sTNFRI as the two relevant factors expressed in increased amounts in culture supernatants from ADAM-9$^{-/-}$ fibroblasts. TIMP-1 was associated with induced melanoma cell proliferation, whereas soluble TNFR1 mediated the reduced cellular apoptosis *in vitro*. *In vivo*, injection of murine melanoma cells into the flank of ADAM-9$^{-/-}$ animals resulted in the development of significantly larger tumors than in wild-type animals as a result of increased proliferation and decreased apoptosis of melanoma cells. Taken together, stromal expression of ADAM-9 during melanoma development modulates the expression of TIMP-1 and sTNFR1, which in turn affect tumor cell proliferation and apoptosis.

Journal of Investigative Dermatology (2012) **132,** 2451–2458; doi:10.1038/jid.2012.153; published online 24 May 2012

INTRODUCTION

Development of melanoma is typically initiated in the skin and is frequently followed by recurrence at distant sites. This process involves expression and activity of proteolytic enzymes to degrade basement membranes, migration through the tissue, and modulation of cellular contacts. Enzymes involved in these processes belong to the metallo-, serine, and cysteine proteases produced by either melanoma cells or stromal cells surrounding the tumor, or both (Zigrino *et al.*, 2005a). A family of proteases with a disintegrin and metalloprotease domain (ADAM) has been involved in cancer progression (Duffy *et al.*, 2009). ADAMs shed cell surface molecules having important roles in cancer progression such as TNFR, EFGR, and their ligands (Murphy, 2008). Among those enzymes, ADAM-9 is upregulated in a number of cancers including renal, breast, and prostate cancer (O'Shea *et al.*, 2003; Fritzsche *et al.*, 2008). In prostate cancer, ADAM-9 leads to altered FGF and EFG signaling by cleaving the FGFR2iiib and EGF ligands (Peduto *et al.*, 2005). A further activity ascribed to ADAMs is their ability to mediate cellular interactions with integrin receptors (White, 2003). ADAM-9 has been shown to interact with α6β1 on fibrosarcoma cells (Nath *et al.*, 2000) and with α3β1 integrins on keratinocytes (Zigrino *et al.*, 2007), thereby modulating cell migration. ADAM-9 is also upregulated in human melanoma, where its expression is detected at the tumor–stroma border by both tumor and stromal cells (Zigrino *et al.*, 2005b). In melanoma cells, we have recently shown that ADAM-9 interacts with multiple β1 integrin receptors to mediate interaction with stromal fibroblasts *in vitro* (Zigrino *et al.*, 2011).

Despite the above data, the precise role of host-derived expression of ADAM-9 for the progression and metastasis of melanoma is unclear. To address this question, we used both *in vitro* coculture system of B16F1 melanoma cells and wild-type (WT) or ADAM-9 null fibroblasts (ADAM-9$^{-/-}$) and *in vivo* grafting of murine melanoma cells in animals with genetic ablation of ADAM-9. We provide evidence that two factors , TIMP-1 and soluble TNFR1, are altered upon ADAM-9 ablation and mediate increased proliferation and reduced apoptosis, respectively, in melanoma cells *in vitro*

[1]*Department of Dermatology, University Hospital of Cologne, Cologne, Germany;* [2]*Department of Microbiology, Immunology and Cancer Biology, University of Virginia, Charlottesville, Virginia, USA;* [3]*Department of Dermatology, University of Bonn, Bonn, Germany and* [4]*Hospital for Special Surgery at Weill Medical College of Cornell University, New York, New York, USA*

Correspondence: Paola Zigrino, Department of Dermatology, University Hospital of Cologne, Kerpener Strasse 62, 50937 Cologne, Germany. E-mail: Paola.Zigrino@uni-koeln.de

Abbreviations: ANAs, antinuclear autoantibodies; CM, conditioned media; mRNA, messenger RNA; TNF, tumor necrosis factor; WT, wild-type

Received 5 December 2011; revised 23 March 2012; accepted 24 March 2012; published online 24 May 2012

and *in vivo*. In summary, we have identified ADAM-9 with a role in modulating the proliferation and apoptosis of melanoma cells.

RESULTS

ADAM-9 expression in stromal fibroblasts modulates melanoma cell growth

In murine melanomas, as shown in Figure 1a, ADAM-9 was expressed similarly as observed in human tumors, with ADAM-9 detected in melanoma cells facing the stroma and in peritumoral stromal cells. *In vitro*, coculture of B16F1 murine melanoma cells either in transwell or with conditioned media (CM) prepared from WT or ADAM-9$^{-/-}$ fibroblasts resulted in a significant increase of proliferation when cultured with ADAM-9$^{-/-}$ as compared with WT fibroblasts (Figure 1b). A similar pro-proliferative effect of ADAM-9$^{-/-}$ fibroblast media was detected in BLM, A375, and 530, but not in SKmel28 human melanoma cells (Supplementary Figure 1A online). Interestingly, no altered cell proliferation was detected when other tumor cells, such as glioma (Gli36) or the tumorigenic keratinocyte line (II4rT), were stimulated with CM from both fibroblast genotypes (Supplementary Figure 1A online).

These results indicated that increased melanoma cell proliferation is induced by a soluble factor–mediated mechanism. To identify the soluble factors secreted by fibroblasts that could influence B16F1 melanoma cell proliferation, supernatants from WT and ADAM-9$^{-/-}$ fibroblast were analyzed by a mouse cytokine antibody array. A prominent increase of TIMP-1, sTNF-α, and sTNFRI in supernatants from ADAM-9$^{-/-}$ fibroblasts was observed compared with WT fibroblasts (Figure 2a).

Increased expression of TIMP-1 was also detected in supernatants of ADAM-9$^{-/-}$ fibroblasts analyzed by immunoblot; one representative culture is shown for each genotype (Figure 2b). In addition, semiquantitative reverse transcriptase PCR analysis of TIMP-1 from ADAM-9$^{-/-}$ and WT fibroblasts showed increased TIMP-1 transcript levels in ADAM-9$^{-/-}$ versus WT fibroblasts (Figure 2b).

ELISA results showed an increase of intracellular and secreted tumor necrosis factor (TNF)-α in ADAM-9$^{-/-}$ as compared with WT fibroblasts (Figure 2c). By western blot analysis, we could also detect increased amounts of soluble TNFRI in the supernatant from ADAM-9$^{-/-}$ fibroblasts (Figure 2d). Two forms were identified, the 55-KDa, exosome-associated TNFRI (ex-TNFRI) (Feras *et al.*, 2004)

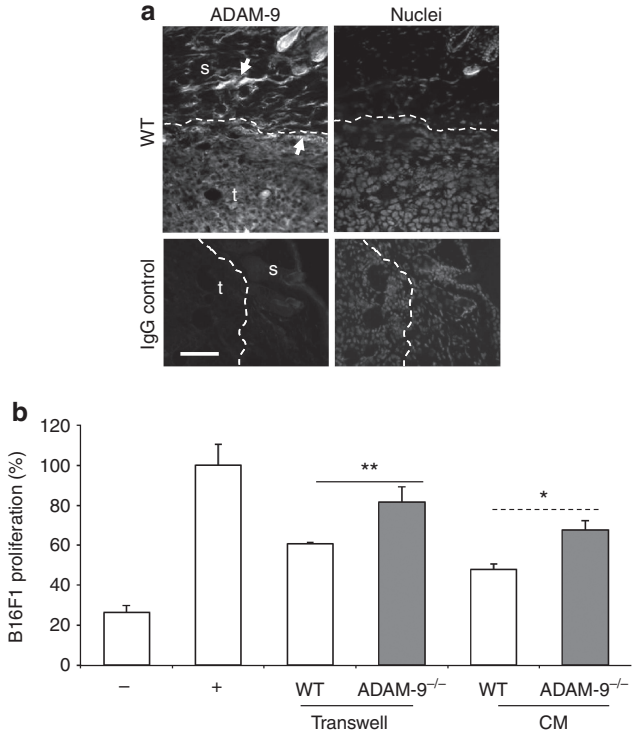

Figure 1. ADAM-9 expression in murine melanoma. (**a**) ADAM-9 detection in B16F1 melanomas grown in mice. ADAM-9 expression in melanoma at the tumor–stroma border is indicated by the arrow. IgGs were used as control. Dashed lines denote the tumor–stroma border. s, stroma; t, tumor. Scale bar = 200 μm. (**b**) B16F1 proliferation after coculture with wild-type (WT) or ADAM-9$^{-/-}$ fibroblasts either in transwell or with conditioned media (CM). The average proliferation of cells cultured with 10% serum (+) was set to 100%, and cell proliferation in the presence of WT or ADAM-9$^{-/-}$ fibroblasts or fibroblast CM was calculated as a ratio of this value. Serum-free control is indicated by (–). The graph represents mean ± SD. *P<0.05, **P<0.001.

a

	WT	ADAM-9$^{-/-}$
GM-CSF	3.44	2.53
CRG-2	0.55	0.61
TIMP-1	3.61	28.59
sTNF-α	1.32	4.19
sTNFRI	1.65	52.78
IFNγ	2.00	0.57
IL-6	2.05	6.50
IL-1α	7.59	15.35

c

TNF-α (pg ml^{-1})		
	Supernatant	Lysate
WT	34.8 ± 5.9	20.2 ± 12.9
ADAM-9$^{-/-}$	46.6 ± 6.7	55.2 ± 38.3

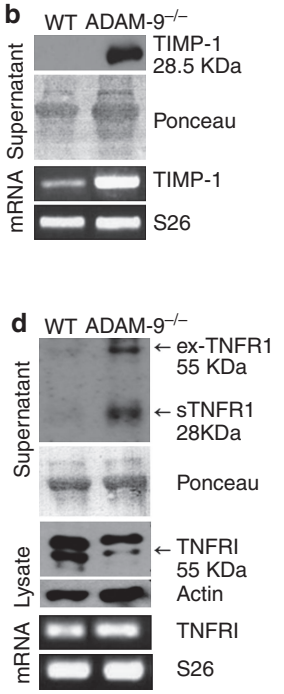

Figure 2. TIMP-1 enhances B16F1 proliferation. (**a**) Expression of soluble factors in fibroblast supernatants using a mouse cytokine antibody array. Shown are arbitrary units/biotin-conjugated IgG-positive control. (**b**) Analysis of TIMP-1 protein in supernatants from fibroblasts. Ponceau was used to ensure loading/transfer. Shown is a representative blot (n = 5 per genotype). Reverse transcriptase PCR (RT–PCR) amplification of the TIMP-1 transcript. Shown is a representative amplification (n = 8 per genotype). (**c**) Quantification of tumor necrosis factor (TNF)-α in fibroblasts by ELISA (n = 4 per genotype). Values are expressed as mean ± SD. (**d**) Analysis of TNFRI in fibroblasts. Shown is one representative analysis out of two using five different fibroblast preparations per genotype. Ponceau and actin were used as controls. S26 was used as internal control for RT–PCR. mRNA, messenger RNA; WT, wild type.

and the 28-KDa shed form (sTNFRI), with a parallel decrease of the membrane-bound form (Figure 2d). In addition, no alteration in TNFRI transcripts was detected in both fibroblast genotypes (Figure 2d).

TIMP-1 enhances melanoma cell proliferation

Incubation of B16F1 cells with recombinant TIMP-1 for 24 hours resulted in a significant increase in cell proliferation compared with that under serum-free conditions (Supplementary Figure 1B online). Increased proliferation was also detected in human melanoma cells stimulated with the recombinant TIMP-1 (Supplementary Figure 1B online), suggesting a common mechanism of induction.

To investigate whether increased TIMP-1 detection in fibroblasts media is responsible for the induction of murine melanoma cells proliferation in coculture, we neutralized TIMP-1 in the supernatant from ADAM-9$^{-/-}$ fibroblasts before melanoma treatment. Blocking the activity of TIMP-1 using neutralizing antibodies led to abolishment of the induced melanoma cell proliferation, which was now comparable to those detected upon cell stimulation with the supernatant from WT fibroblasts (Figure 3a).

ADAM-9 depletion in fibroblasts leads to reduced melanoma cell apoptosis

Stimulation of B16F1 cells with CM from ADAM-9$^{-/-}$ fibroblasts resulted not only in a significant increase in proliferation (Figure 1b) but also in a concomitant reduction of B16F1 apoptosis compared with cells stimulated with WT supernatants (Figure 3b). Despite being tumor cells, B16F1 cells treated with TNF undergo the apoptosis process, indicating that they are still sensitive to apoptosis induction (Figure 3b). As shown in Figure 3c, neutralization of TIMP-1 in ADAM-9$^{-/-}$ fibroblast media had no effect on B16F1 apoptosis, thus excluding TIMP-1 as the factor mediating the anti-apoptotic effect observed.

Two additional proteins that we found alternatively secreted/processed in the media of ADAM-9$^{-/-}$ fibroblasts, namely sTNF-α and sTNFRI (Figure 2a, c, and d), have been shown to exert an important role in apoptotic processes (Chen and Goeddel, 2002).

To investigate whether blocking sTNFRI release from cell surface, which we found increased in ADAM-9$^{-/-}$ fibroblast supernatants, would abolish the detected reduced apoptosis in B16F1, we have treated ADAM-9$^{-/-}$ fibroblasts with TAPI-0, a metalloproteinase inhibitor, before melanoma cell treatment. TAPI-0 treatment led to efficient inhibition of TNFRI shedding, and the soluble form of the receptor was now undetectable in fibroblast supernatants (Figure 4a). Furthermore, reduced release of TNFRI was paralleled by increased detection of the membrane-bound form. Stimulation of B16F1 cells with supernatant from TAPI-0-treated ADAM-9$^{-/-}$ fibroblasts led to a significant increase in B16F1 cell apoptosis; this effect could be blocked when, in addition, we also supplied recombinant soluble TNFRI to the media (Figure 4a). These results support the antagonistic role of increased sTNFRI in ADAM-9$^{-/-}$ fibroblasts in mediating suppression of B16F1 apoptosis.

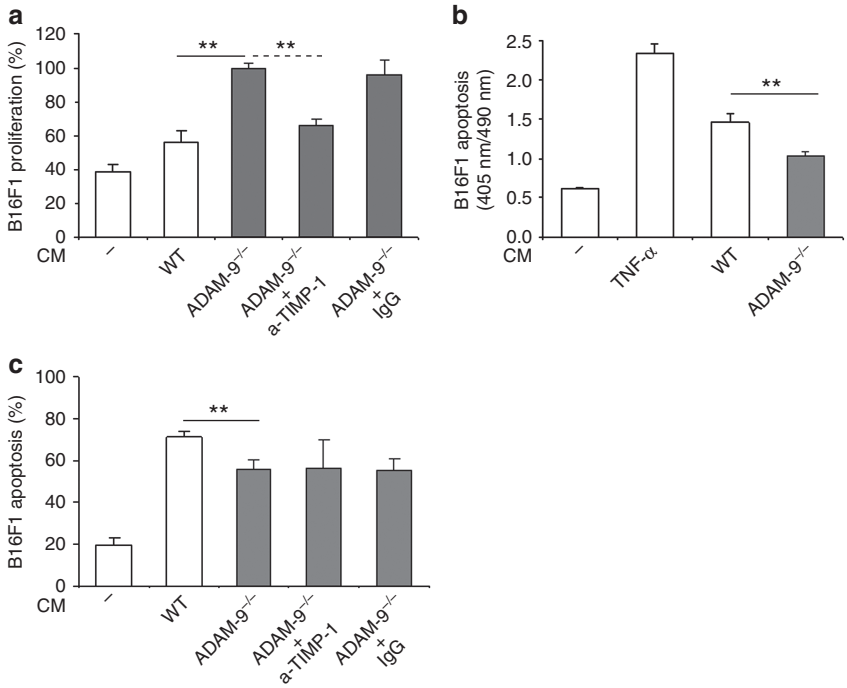

Figure 3. TIMP-1 influences B16F1 proliferation but not apoptosis. (**a**) B16F1 cell proliferation in the presence of conditioned media (CM) from fibroblasts with/without anti-TIMP-1 or IgG control antibodies (2 μg ml^{-1}, a-TIMP-1). Cell proliferation in the presence of ADAM-9$^{-/-}$ supernatant was set as 100%. $^{**}P<0.005$. B16F1 cell apoptosis in the presence of c.m. from fibroblasts without (**b**) or with (**c**) anti-TIMP-1 or IgG control antibodies (2 μg ml^{-1}, a-TIMP-1). Values are expressed as percentage relative to the 100% reference value (cell apoptosis in the presence of 100 ng ml^{-1} recombinant TNF-α). $^{*}P<0.05$; $^{**}P<0.008$. All data represent mean ± SD, and graphs are representative of three independent experiments. TNF-α, tumor necrosis factor; WT, wild type.

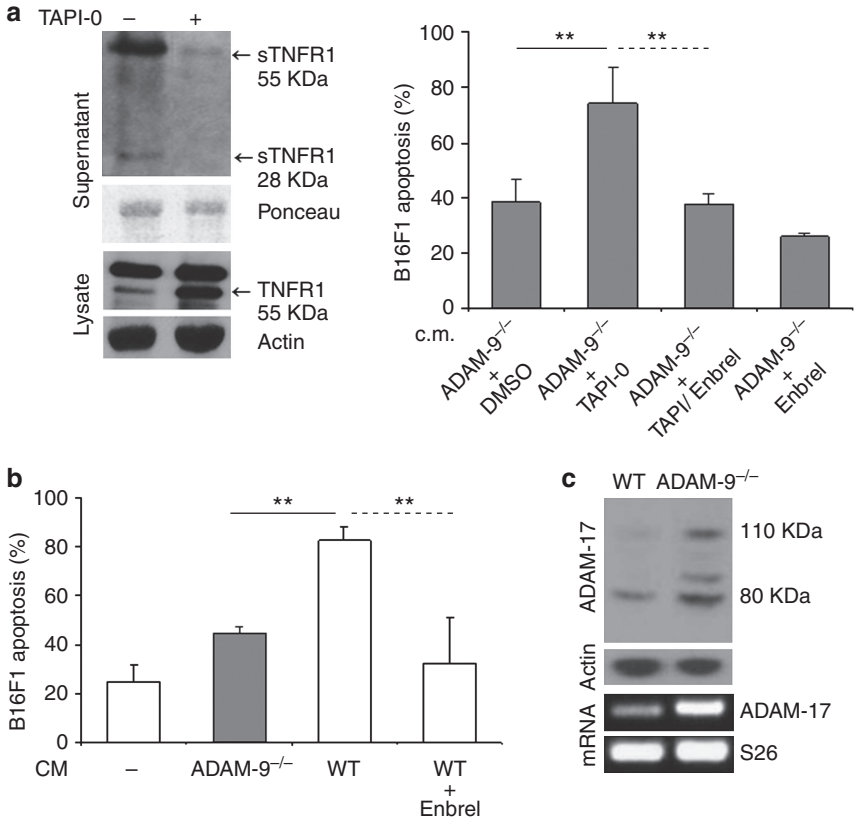

Figure 4. Shedding of TNFRI in fibroblasts influences B16F1 apoptosis. (**a**) Left, immunoblot analysis of soluble TNFRI in ADAM-9$^{-/-}$ fibroblasts in the absence/presence of TAPI-0 (10 μM). Ponceau and actin served as controls. Right, apoptosis of B16F1 cells stimulated with ADAM-9$^{-/-}$ fibroblast supernatant after treatment with TAPI-0, DMSO (control), or with Enbrel (5 μg μl^{-1}). Alternatively, (**b**) B16F1 cell apoptosis was analyzed after treatment of WT fibroblast supernatants with/without Enbrel (recombinant soluble TNFR1). B16F1 cell apoptosis in the presence of recombinant tumor necrosis factor (TNF)-α was set as 100%. Data represent mean ± SD. $^{**}P<0.003$. (**c**) ADAM-17 protein and transcripts were analyzed in fibroblasts. Shown is one representative analysis out of two performed with four different fibroblast preparations per genotype. S26 and actin served as controls. CM, conditioned media; mRNA, messenger RNA; WT, wild type.

Culture of B16F1 cells with supernatant from WT fibroblasts in the presence of recombinant soluble TNFRI (Enbrel) significantly reduced B16F1 cell apoptosis, mimicking the anti-apoptotic effect of the supernatant from ADAM-9$^{-/-}$ fibroblasts on B16F1 cells (Figure 4b).

The release of TNFRI from the cell surface has been shown to be mainly mediated by the activity of TACE/ADAM-17 (Bell *et al.*, 2007). By reverse transcriptasePCR analysis of ADAM-17 transcripts in ADAM-9-null fibroblasts, we detected an ~2-fold upregulation as compared with WT (Figure 4c). Increase in transcripts was paralleled by increased expression of ADAM-17 protein in both pro and active forms in lysates of ADAM-9-depleted fibroblasts as compared with WT cells (Figure 4c).

To support the causal role of ADAM-17, we silenced ADAM-17 in ADAM-9-null fibroblasts. We obtained efficient downregulation with the most prominent transcriptional effect (80%) when using 150 pmol of the small interfering RNA (Supplementary Figure 3A online). A less prominent, 20%, reduction of pro and active forms of ADAM-17 was instead detected by immunoblot (Supplementary Figure 3B online). Silencing of ADAM-17 in ADAM-9$^{-/-}$ fibroblasts also resulted in a 30% reduction in 28-KDa shed TNFR (Supplementary Figure 3C online), and stimulation of B16F1 cells with supernatant from silenced ADAM-9$^{-/-}$ fibroblasts led to a small but significant increase in B16F1 cell apoptosis (Supplementary Figure 3D online).

ADAM-9$^{-/-}$ ablation in mice results in enhanced melanoma growth

To translate our *in vitro* findings *in vivo*, we analyzed the growth of B16F1 melanoma cells in WT mice and mice lacking ADAM-9. B16F1 melanoma cells were injected intradermally into the flank of WT or ADAM-9$^{-/-}$ mice. Tumor growth/size was measured as a function of time. Measurable tumors were detected as early as 6 days post B16F1 injection and reached an average size of 34.3 mm^3 in WT animals, whereas depletion of ADAM-9 resulted in significantly increased tumor size up to 4-fold, with an average size of 131.2 mm^3 (Figure 5a). At day 13, 42% of ADAM-9$^{-/-}$ mice had tumors larger than 1 cm^3, in contrast to the WT mice with only 11% of tumors larger than 1 cm^3 (Figure 5a). A similar difference in tumor growth was also detected when we used B16F0 cells and tumor explants from the Hgf-Cdk4^{R24C} mice (data not shown; Tormo *et al.*, 2006). *In vivo*, analysis of ADAM-9 messenger RNA transcripts in

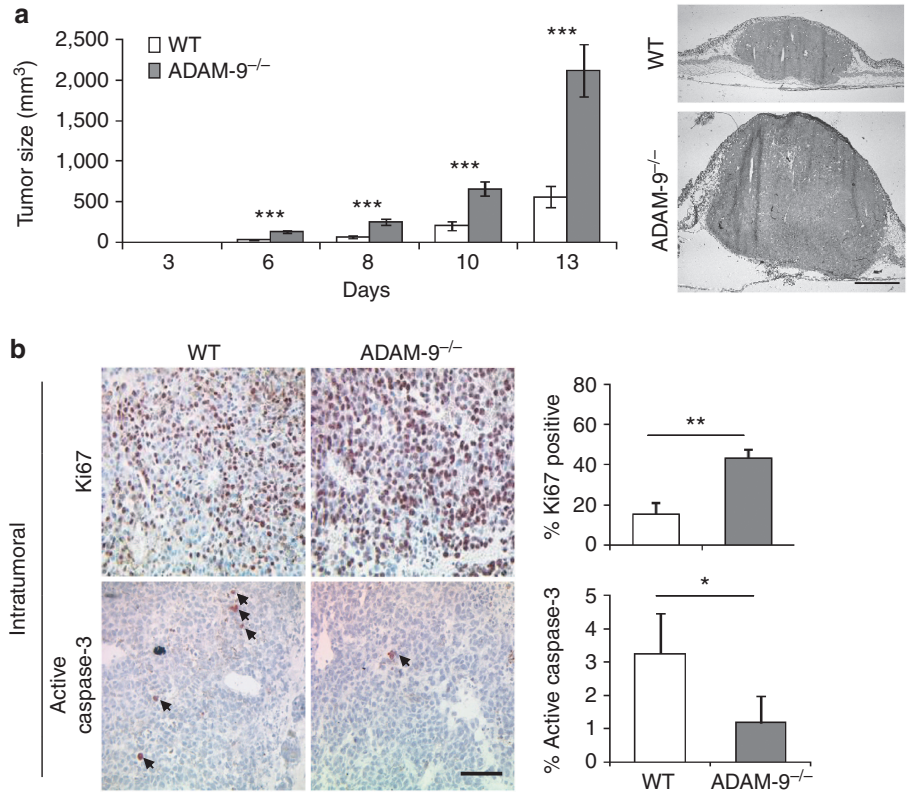

Figure 5. Depletion of host-derived ADAM-9 favors tumor growth. (**a**) Tumor size was measured over time after injection of B16F1 melanoma cells into the flank of wild type (WT) or ADAM-9$^{-/-}$ mice (day 3, $n=26$; day 6, $n=20$; day 8 and day 10, $n=16$; day 13, $n=12$). Data are presented as average tumor volume ± SEM. ***$P<0.0001$. Representative sections of day-13 tumors, stained with hematoxylin–eosin, are shown. Scale bar = 25 μM. (**b**) Immunodetection of Ki67 and active caspase-3-positive melanoma cells. Positive cells were counted in three fields within the tumor and expressed as a percentage of the total number ($n=7$). Values are expressed as mean ± SEM; *$P<0.05$; **$P<0.005$. Scale bar = 200 μm.

B16F1 tumors developed either in WT or ADAM-9$^{-/-}$ animals showed increased expression in tumors grown in the WT and ADAM-9$^{-/-}$ hosts as compared with healthy skin, although this was more abundant in the WT mice (Supplementary Figure 2 online).

Melanoma cell proliferation *in vivo* was altered as indicated by the 2.5-fold increase in the average number of Ki67-positive cells within the tumors of ADAM-9$^{-/-}$ animals at day 13 post injection as compared with those developed in WT littermates (Figure 5c, upper panel). Similarly, quantification of the number of active caspase-3-positive melanoma cells in the same specimens showed a significant (2.7-fold) reduction in the number of apoptotic melanoma cells in ADAM-9$^{-/-}$ animals as compared with WT (Figure 5c).

Analysis of tumor-infiltrating T-/B-cells, neutrophils, and macrophages showed no significant difference in the infiltrated cells in melanomas developed in WT or ADAM-9$^{-/-}$ mice. We failed to detect any alterations in the number of vessels formed around the tumors in both animals (data not shown). These results suggest that increased tumor growth in ADAM-9$^{-/-}$ animals is the result of an altered balance between proliferation and apoptosis upon tumor–stroma communication.

Analysis of TIMP-1, sTNF-α, and sTNFRI in extracts from melanomas by antibody array indicated increased amounts, similar to those detected *in vitro* (Figure 2), of all three proteins in the tumor from ADAM-9$^{-/-}$ as compared with WT mice (Figure 6a). *In vivo*, we detected increased TIMP-1 in elongated fibroblast-like cells in the peritumoral stroma, whereas very little expression was observed in the peritumoral stroma of tumors from WT littermates (Figure 6b, lower panel). Accordingly, increased B16F1 melanoma cell proliferation was also detected in the tumor periphery, facing the stroma, in tumors from ADAM-9$^{-/-}$ (Figure 6b) as compared with WT mice.

DISCUSSION

ADAM-9 is a multidomain metalloprotease that has been shown to be upregulated in a number of cancers (O'Shea *et al.*, 2003; Fritzsche *et al.*, 2008). In melanoma developed in mice, ADAM-9 expression is observed at the tumor–stroma border in stromal and tumor cells, an expression pattern that resembles that observed in primary human melanoma (Zigrino *et al.*, 2005b). Even though we could show that ADAM-9 expression by both melanoma cell and stromal fibroblasts may mediate cellular interactions (Zigrino *et al.*, 2011), a role for the fibroblast-specific expression of ADAM-9 during melanoma development remained elusive. To analyze how ADAM-9 expression in fibroblasts influences melanoma growth, we used *in vitro* coculture systems of melanoma cells

a

	WT	ADAM-9$^{-/-}$
TIMP-1	2.88	19.35
sTNF-α	4.7	26.21
sTNFRI	15.48	56.65

b

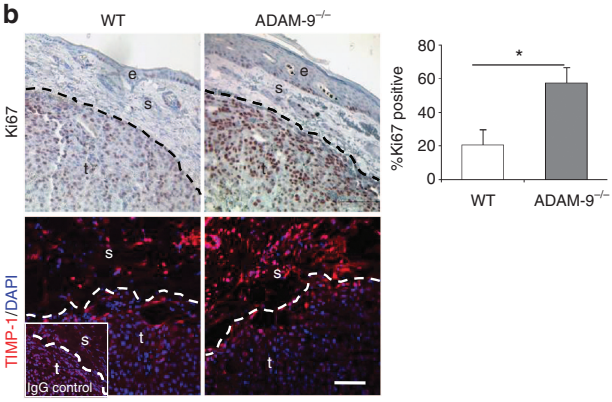

Figure 6. Expression of TIMP-1 in murine melanoma. (**a**) Expression of TIMP-1, tumor necrosis factor (TNF)-α, and TNFRI in lysates from tumors of wild-type (WT) and ADAM-9$^{-/-}$ mice detected using a mouse cytokine antibody array. Shown are arbitrary units per biotin-conjugated IgG control. (**b**) Tumor cell proliferation at the tumor periphery was assessed by counting the number of Ki67-positive cells in three fields and expressed as percentage of the total number of cells. The average number is shown as mean ± SEM. *$P<0.05$. TIMP-1 (red) was analyzed in tumor sections; the nuclei are stained in blue. IgGs were used as control. Dashed lines indicate tumor–stroma border. e, epidermis; s, stroma; t, tumor. Scale bar = 200 μm.

and fibroblasts isolated from WT or ADAM-9$^{-/-}$ mice. Interestingly, direct (transwell) or indirect (CM) coculture of B16F1 cells with ADAM-9$^{-/-}$ and WT dermal fibroblasts led to a significant induction of proliferation, paralleled by a reduction of apoptotic cells. These data indicated that soluble factors secreted or released from the cell surface from ADAM-9$^{-/-}$ fibroblasts have the potential to modulate the growth of melanoma cells. TIMP-1 was among those factors altered in ADAM-9$^{-/-}$ fibroblasts *in vitro*. Neutralization of TIMP-1 abolished the increased melanoma cell proliferation observed upon stimulation with supernatant from ADAM-9$^{-/-}$ fibroblasts. The growth-promoting activity of TIMP-1 was not only limited to murine melanoma cells but was also found with human melanoma cells, suggesting that the observed event may be important also in the context of human disease. The activity of TIMP-1 in cancer is quite controversial, being either a promoter (Yoshiji *et al.*, 1998) or an inhibitor of tumor growth (Soloway *et al.*, 1996). Recent reports demonstrated that TIMP-1 regulates cell proliferation in colorectal cancer cells and premalignant melanocytes, although the molecular mechanisms of this regulation are still not known (Sorensen *et al.*, 2008; Ricca *et al.*, 2009). Despite the fact that TIMP-1 also has anti-apoptotic activity (Stetler-Stevenson, 2008), neutralization of TIMP-1 in CM from ADAM-9$^{-/-}$ fibroblasts did not affect apoptosis of stimulated melanoma cells. Two additional factors identified as increased in ADAM-9$^{-/-}$ fibroblast supernatants were TNF-α, a cytokine that exerts antitumor immunity by binding to TNFRI (Chen and Goeddel, 2002; Calzascia *et al.*, 2007), and soluble TNFRI. Binding of soluble TNF-α to soluble TNFRI antagonizes binding to the membrane receptor, thus impeding transduction, leading to apoptosis (Engelmann *et al.*, 1989; Chen and Goeddel, 2002). We believe that in our system this mechanism is responsible for the reduced apoptosis detected in melanoma cells. Soluble TNFRI is released by ectodomain shedding (Hikita *et al.*, 2009), and ADAM-17 has been identified as the main sheddase in this process (Bell *et al.*, 2007). Interestingly, we found ADAM-17 upregulated in fibroblasts from ADAM-9-null animals, thus suggesting that the increase in sTNFRI maybe due to the observed increase in ADAM-17. Downregulation of ADAM-17 by RNA silencing or inhibition of proteolytic activity with TAPI-0 in ADAM-9$^{-/-}$ fibroblasts led to reduced sTNFRI shedding and in turn to increased apoptosis of stimulated B16F1 cells. Thus, taken together, we suggest that increased expression and activity of ADAM-17 may mediate the proteolytic release of sTNFRI, which binds TNF and leads to decreased B16F1 apoptosis upon stimulation with ADAM-9$^{-/-}$ fibroblast supernatant.

In the absence of ADAM-9, altered production of TIMP-1 and TNF-α may be the result of an altered notch signaling. One explanation for this may be the persistence of notch signaling as a result of reduced Delta-Like ligand-1 (Dll-1) cleavage in the absence of enzymatic activity of ADAM-12 and -9 (Dyczynska *et al.*, 2007; Zolkiewska, 2008).

To analyze the implications for our *in vitro* finding *in vivo*, we grafted B16F1 melanoma cells in the flank of WT and ADAM-9$^{-/-}$ mice. As predicted by the pro-proliferative and anti-apoptotic effect, which we detected in ADAM-9$^{-/-}$ fibroblasts toward B16F1 melanoma cells *in vitro*, we observed increased tumor growth in mice lacking ADAM-9. In line with our *in vitro* data, also *in vivo* we detected a significant increase in tumor cell proliferation in melanoma developed in ADAM-9$^{-/-}$ mice, while apoptosis was reduced. In addition, *in vivo* we could detect increased expression of sTNF-α and sTNFRI in tumors from ADAM-9$^{-/-}$ mice. A similar increase was also found in the levels of TIMP-1, which localizes in fibroblasts at the tumor–stroma border in melanoma from ADAM-9$^{-/-}$ mice facing a more proliferative melanoma cell front.

Interestingly, in contrast with our results, using another melanoma cell line, B16F0, Guaiquil *et al.* (2009) have shown that tumor growth of injected cells was reduced in ADAM-9$^{-/-}$ mice compared with controls. One possible explanation for the difference between our results and those of Guaiquil and colleagues (2009) is that in their studies the tumor cells were injected subcutaneously, whereas we used intradermal injections in our study. This raises the possibility that the contribution of ADAM-9 to the tumor environment is dependent on the site. Further studies will be necessary to confirm the reason for such a discrepancy.

In summary, we have shown *in vitro* and *in vivo* that stromal-derived ADAM-9 is important during the development of melanoma, and identified two molecular targets of ADAM-9 that modulate melanoma cell proliferation and apoptosis, namely TIMP-1 and TNF-α/sTNFR1.

MATERIALS AND METHODS

Cells, cell culture, and preparation of CM

Murine dermal fibroblasts were isolated from newborn skin of WT and ADAM-9$^{-/-}$ mice as previously described (Florin *et al.*, 2006). Isolated fibroblasts, characterized on the basis of their morphological appearance, were used between passages 2 and 4 for experiments. For the preparation of fibroblast supernatants, cells were cultured until 90% confluent, washed twice with phosphate-buffered saline, and cultured with serum-free DMEM with or without 10 μM TAPI-0 (Biomol, Hamburg, Germany) for 24 hours. The supernatant was centrifuged at 2,000*g* for 5 minutes, to remove cellular debris, and transferred to new tubes. B16F1 murine melanoma cells were cultured in DMEM containing 10% fetal calf serum, penicillin, and streptomycin. Further information including ELISA and antibody array is provided in the Supplementary Methods online.

Proliferation and apoptosis assays

Cell proliferation was assessed using the Cell Proliferation ELISA kit (Roche diagnostics, Mannheim, Germany), which measures the incorporation of BrdU into DNA, according to the manufacturer's instructions.

Apoptosis was quantified using cell death detection ELISA (Roche diagnostics). This assay detects the amount of cytoplasmic oligonucleosomes released after DNA cleavage, using a combination of anti-histone and anti-DNA capture and detection antibodies. Recombinant mouse TNF-α (Miltenyi Biotec, Bergisch Gladbach, Germany) at a concentration of 100 ng ml^{-1} was used to induce cell apoptosis. For neutralization experiments, supernatants were preincubated with anti-TIMP-1 antibody or IgG control or 5 μg ml^{-1} Enbrel (Wyeth Pharma, Münster, Germany) for 30 minutes at room temperature before stimulating cells.

Tumor growth assay *in vivo*

B16F1-GFP and B16F0 murine melanoma cells (1×10^6 cells) in 0.1 ml phosphate-buffered saline or transplantable melanoma cells from Hgf-Cdk4^{R24C} mice were injected intradermally into the flank of 6- to 8-week old, WT and ADAM-9$^{-/-}$ littermate mice as previously described (Zigrino *et al.*, 2009). These animals are of mixed genetic background (129/SvJ and C57BL/6J); however, to reduce variations in the backgroud and to increase the number of animals needed for the analysis, collected offspring of *Adam9*$^{-/-}$ or WT from one pair of heterozygous *Adam9*$^{+/-}$ parents were mated with one another to generate litters of WT or *Adam9*$^{-/-}$ mice ($n = 26$ for each genotype) that were closely related, as derived from the same heterozygous grandparents. Tumor size was measured every 2 days using a precision caliper (Mitutoyo, Neuss, Germany), and volume calculated by multiplying length, width, and depth, which was expressed as mean ± SEM. Animals were killed at day 3, 6, 10, and 13 post injection. The animal experiments were approved by the local veterinary authority (NRW authorization 50.203.2-K 37a, 20/05).

Immunohistochemistry and immunofluorescence analysis

Tumors were removed surgically at the indicated time point; one half was embedded in optimal cutting temperature compound (O.C.T, Vogel, Giessen, Germany) and frozen, and the other half was fixed in 1% formalin and embedded in paraffin. Sections (8 μm thick) were cut and processed for immunofluorescence and immunohistochemistry analysis. Further information is supplied in the Supplementary Methods online.

Western blot analysis

CM was concentrated by trichloroacetic acid precipitation and solubilized in Laemmli sample buffer. Equal amount of proteins were separated by SDS-PAGE on 10 to 15% (w/v) polyacrylamide gels under reducing conditions, transferred to a Hybond-C Extra membrane (Amersham Biosciences, Freiburg, Germany), and incubated with the primary antibodies overnight at 4 °C. Bound antibodies were detected with horseradish peroxidase–labeled secondary antibody (Dako) and enhanced chemiluminuescence (ECL) reaction.

RNA isolation and amplification

Total RNA from tissues was isolated as previously described (Zigrino *et al.*, 2009). Primers for the amplification of murine ADAM-9, -17, and S26 were described elsewhere (Zigrino *et al.*, 2009; Mauch *et al.*, 2010). The primers used for amplification of murine TIMP-1 and TNFRI were as follows: TIMP-1 sense 5′-CTGGCATCCT CTTGTTGCTA-3′, antisense 5′-AGGGATCTCCAGGTCCACAA-3′, TNFRI sense 5′-GGCAGAGGAGCCTAGTTG-3′, antisense 5′-CACA CCCAGGAACAGTCC-3′. Further information is supplied in the Supplementary Methods.

Statistical analysis

All experiments were performed at least three times in triplicates unless otherwise indicated. Statistical analysis of the data was performed using Student's *t*-test. Differences with $P < 0.05$ were considered statistically significant.

CONFLICT OF INTEREST

The authors state no conflict of interest.

ACKNOWLEDGMENTS

This work was supported by the Melanoma Research Network of the Deutsche Krebshilfe (Melanoma Verbund to P.Z. and C.M.).

SUPPLEMENTARY MATERIAL

Supplementary material is linked to the online version of the paper at http://www.nature.com/jid

REFERENCES

Bell JH, Amy HH, Li Y *et al.* (2007) Role of ADAM17 in the ectodomain shedding of TNF-α and its receptors by neutrophils and macrophages. *J Leukoc Biol* 82:173–6

Calzascia T, Pellegrini M, Hall H *et al.* (2007) *J Clinl Invest* 117:3833–45

Chen G, Goeddel DV (2002) TNF-R1 signaling: a beautiful pathway. *Science* 296:1634–5

Duffy MJ, McKiernan E, ÓDonovan N *et al.* (2009) Role of ADAMs in cancer formation and progression. *Clin Cancer Res* 15:1140–4

Dyczynska E, Sun D, Yi H (2007) Proteolytic processing of Delta-like 1 by ADAM proteases. *J Biol Chem* 282:436–44

Engelmann H, Aderka D, Rubinstein M *et al.* (1989) A tumor necrosis factor-binding protein purified to homogeneity from human urine protects cells from tumor necrosis factor toxicity. *J Biol Chem* 264:11974–80

Feras HI, Rouhani FN, Cui X *et al.* (2004) Release of full-length 55 KDa TNF receptor 1 in exosome-like vesicles: a mechanism for generation of soluble cytokine receptors. *Proc Natl Acad Sci USA* 101:1297–302

Florin L, Knebel J, Zigrino P *et al.* (2006) Delayed wound healing and epidermal hyperproliferation in mice lacking JunB in the skin. *J Invest Dermatol* 126:902–11

Fritzsche FR, Wassermann K, Jung M *et al.* (2008) ADAM9 is highly expressed in renal cell cancer and is associated with tumour progression. *BMC Cancer* 8:179–88

Guaiquil V, Swendeman S, Yoshida T *et al.* (2009) ADAM9 is involved in pathological retinal neovascularization. *Mol Cell Biol* 29:2694–703

Hikita A, Tanaka N, Yamane S *et al.* (2009) Involvement of a disintegrin and metalloproteinase 10 and 17 in shedding of tumor necrosis factor-alpha. *Biochem Cell Biol* 87:581–93

Mauch C, Zamek J, Abety AN *et al.* (2010) Accelerated wound repair in ADAM-9 knockout animals. *J Invest Dermatol* 130:2120–30

Murphy G (2008) The ADAMs: signalling scissors in the tumour microenvironment. *Nat Rev Cancer* 12:929–41

Nath D, Slocombe PM, Webster A *et al.* (2000) Meltrin gamma (ADAM-9) mediates cellular adhesion through alpha(6)beta(1)integrin, leading to a marked induction of fibroblast cell motility. *J Cell Sci* 113: 2319–28

O'Shea C, McKie N, Buggy Y (2003) Expression of ADAM-9 mRNA and protein in human breast cancer. *Int J Cancer* 105:754–61

Peduto L, Reuter VE, Shaffer DR *et al.* (2005) Critical function for ADAM9 in mouse prostate cancer. *Cancer Res* 65:9312–9

Ricca TI, Liang G, Suenaga AP *et al.* (2009) Tissue inhibitor of metalloproteinase 1 expression associated with gene demethylation confers anoikis resistance in early phases of melanocyte malignant transformation. *Transl Oncol* 2:329–40

Soloway PD, Alexander CM, Werb Z *et al.* (1996) Targeted mutagenesis of Timp-1 reveals that lung tumor invasion is influenced by Timp-1 genotype of the tumor but not by that of the host. *Oncogene* 13: 2307–14

Sorensen NM, Sorensen IV, Wurtz SO *et al.* (2008) Biology and potential clinical implications of tissue inhibitor of metalloproteinases-1 in colorectal cancer treatment. *Scand J Gastroenterol* 43:774–86

Stetler-Stevenson WG (2008) Tissue inhibitors of metalloproteinases in cell signaling: metalloproteinase-independent biological activities. *Sci Signal* 1:re6

Tormo D, Ferrer A, Gaffal E *et al.* (2006) Rapid growth of invasive metastatic melanoma in carcinogen-treated hepatocyte growth factor/scatter factor-transgenic mice carrying an oncogenic CDK4 mutation. *Am J Pathol* 169:665–72

White JM (2003) ADAMs: modulators of cell-cell and cell-matrix interactions. *Curr Opin Cell Biol* 15:598–606

Yoshiji H, Harris SR, Raso E *et al.* (1998) Mammary carcinoma cells over-expressing tissue inhibitor of metalloproteinase-1 show enhanced vascular endothelial growth factor expression. *Int J Cancer* 75:81–7

Zigrino P, Loffek S, Mauch C (2005a) Tumor-stroma interactions: their role in the control of tumor cell invasion. *Biochimie* 87:321–8a

Zigrino P, Mauch C, Fox JW *et al.* (2005b) ADAM-9 expression and regulation in human skin melanoma and melanoma cell lines. *Int J Cancer* 116:853–9b

Zigrino P, Kuhn I, Bäuerle T *et al.* (2009) Stromal expression of MMP-13 is required for melanoma invasion and metastasis. *J Invest Dermatol* 129:2686–93

Zigrino P, Nischt R, Mauch C (2011) The disintegrin-like and cysteine-rich domains of ADAM-9 mediate interactions between melanoma cells and fibroblasts. *J Biol Chem* 286:6801–7

Zigrino P, Steiger J, Fox JW *et al.* (2007) Role of ADAM-9 Disintegrin-cysteine-rich domains in human keratinocyte migration. *J Biol Chem* 282:30785–93

Zolkiewska A (2008) ADAM proteases: ligand processing and modulation of the Notch pathway. *Cell Mol Life Sci* 65:2056–68